Matrik: Jurnal Manajemen, Teknik Informatika, dan Rekayasa Komputer
Vol. 22, No. 1, November 2022, pp. 1∼12
ISSN: 2476-9843, accredited by Kemenristekdikti, Decree No: 200/M/KPT/2020
DOI: 10.30812/matrik.v22i1.1654

Combination Contrast Stretching and Adaptive Thresholding for Retinal Blood Vessel Image

Anita Desiani[1], Irmeilyana[2], Irvan Andrian[3], Endro Setyo Cahyono[4], Des Alwine Zayanti[5], Muhammad Arhami[6], Sugandi Yahdin[7]
[1,2,3,4,5,7] Universitas Sriwijaya, Palembang, Indonesia
[6] Politeknik Lhokseumawe, Aceh, Indonesia

Article Info

Article history:

Received December 31, 2021
Revised April 05, 2022
Accepted April 21, 2022

Keywords:

Adaptive Thresholding
Blood Vessel
Contrast Stretching
Drive
Retinal Image
Stare

ABSTRACT

To diagnose diabetic retinopathy is to segment the blood vessels of the retinal, but the retinal images in the DRIVE and STARE datasets have varying contrast, so the enhancement is needed to obtain a stable image contrast. In this study, image enhancement was performed using the Contrast Stretching and continued with segmentation using the Adaptive Thresholding on retinal images. The image that has been extracted with green channels will be enhanced with Contras Stretching and segmented with Adaptive Thresholding to produce a binary image of retinal blood vessels. The purpose of this study was to combine image enhancement techniques and segmentation methods to obtain valid and accurate retinal blood vessels. The test results on DRIVE were 95.68 for accuracy, 65.05% for sensitivity, and 98.56% for specificity. The test results of Adam Hoover's ground truth on STARE were 96.13% for, 65.90% for sensitivity, and 98.48% for specificity. The test results for Valentina Kouznetsova's ground truth on the STARE were 93.89% for accuracy, 52.15% for sensitivity, and 99.02% for specificity. The conclusion obtained is that the processing results on the DRIVE and STARE datasets are very good with respect to their accuracy and specificity values. This method still needs to be developed to be able to detect thin blood vessels with the aim of being able to improve and increase the sensitivity value obtained.

Corresponding Author:

Anita Desiani,
Mathematics and Natural Science Faculty, Department of Mathematics,
Sriwijaya University, Palembang, Indonesia
Email: anita_desiani@unsri.ac.id

How to Cite: A. Desiani, Combination Contrast Stretching and Adaptive Thresholding for Retinal Blood Vessel Image, MATRIK : Jurnal Manajemen, Teknik Informatika dan Rekayasa Komputer, vol. 22, no. 1, pp. 1-12, Nov. 2022.

1. INTRODUCTION

Diabetic retinopathy is one of the leading causes of blindness by cutting the retinal blood vessels in diabetic patients [1]. Early diagnosis of the disease can be detected from the blood vessels because the retinal blood vessels have different branching patterns and sizes. Retinal blood vessels changes can be identified by segmentation of retinal blood vessels with appropriate analysis. It causes retinal blood vessel segmentation is an appropriate way to extract only parts of the blood vessels, retinal blood vessel segmentation can also be used to diagnose various eye diseases [2].

The development of artificial intelligence regarding pattern recognition in digital image processing raises many problems; namely, the results obtained are blurry, unclear, there is a lot of noise, and lack of light, so that the results of digital image processing are less accurate. One method of image enhancement is by using the Contrast Stretching method. The advantage of Contrast Stretching was that it increased the intensity in an image so that the color intensity range was complete [3]. Images with high contrast will be easy to get information, while images with low contrast will be challenging. Image contrast enhancement used the Contrast Stretching method has been carried out by several studies [4, 5]. Research [4] applied Contrast Stretching and Median Filter to retinal images that produced an average PSNR value of 42.13 dB and an MSE of 9.14. In addition, research [5] also applied gray level scale and Contrast Stretching to retinal images with a PSNR value of 42.14 dB and an MSE value of 9.15. Both studies have a PSNR value of more than 40 dB, meaning that using Contrast Stretching can improve image quality for the better [5]. In principle, Contrast Stretching is beneficial for improved image quality or only in the enhancement process but cannot do segmentation. Another method is needed for segmentation, namely Adaptive Thresholding.

In image segmentation, digital image processing is an essential step in the image pattern recognition stage. Segmentation is a process to find the unique characteristics of an image. One of the methods is Adaptive Thresholding, which uses a morphological tracking and filtering scheme. The advantage of the Adaptive Thresholding method is that it can be detected small and large blood vessels simultaneously. The disadvantage of the Adaptive Thresholding method is that it can be only segmented bright quality images, so that the diversity of light intensity can affect this method [6]. Several studies performed segmentation of blood vessels in retinal images, including [7–10]. Research [7] applied the Otsu Thresholding method with image enhancement using the Frangi Filter, which produced an average accuracy and sensitivity value of 96.58% and 97.03% in the DRIVE dataset, while in the STARE dataset, it is 93.76% and 49.7%. Furthermore, research [8] applied Otsu Thresholding with image enhancement using CLAHE and Adaptive Filter obtained accuracy and specificity values of 93.68% and 61.60% on the DRIVE dataset while in the STARE dataset of 94.56% and 97.22%, respectively. Then research [9] applied Hessian Matrix, and Random walks with the results of accuracy and specificity of 93.76% and 98.24%, respectively. In addition, research [10] applied Adaptive Thresholding with image enhancement using CLAHE and 2D-Gabor Filter resulted in an average accuracy and specificity of 91% and 97% on the STARE dataset, respectively. Unfortunately, the four studies still had a low sensitivity value below 65%.

The purpose of this study was to combine image enhancement techniques and segmentation methods to obtain valid and accurate retinal blood vessels. In this study choosed adaptive thresholding for blood vessels segmentation on retinal imaegs. The adaptive threshold was often referred to as the local threshold. Most of the previous studies used global threshold methods such as the Otsu threshold. Otsu Thresholding was a simple method to use in binary segmentation. In fact, adaptive thresholds were computationally more expensive than Otsu thresholds. This was because the adaptive threshold performed segmentation with several different threshold values in several regions in one image. This study focused on the adaptive thresholding method with the aim of increasing the ability of blood vessel segmentation in retinal images by utilizing different threshold values. This was considered that one retinal image has different color intensities for several of its pixels. Using one threshold as a global threshold is inappropriate. The need for adaptive thresholding was a bright picture. That is, the image must had good contrast. For this reason, a method for improving retinal images was needed that focused on methods that make the image had a lighter color intensity. The method was contrast stretching. The combination of contrast stretching and adaptive thresholding was expected to provide a good method that has more accurate and valid results of blood vessel segmentation on retinal images. The study was contained of three stages, the first stage was image enhancement, the second stage was segmentation using adaptive thresholding and the third stage was post processing using morphology and median filter. Image enhancement was a stage to improve image quality. Segmentation was a stage that separated blood vessel fitur on retinal image as foreground with other fiturs as a background. Post processing was a stage to eliminate the remaining noise in the segmented image. The performance results on this study used to evaluate the proposed method were accuracy, sensitivity, and specificity.

2. RESULT AND ANALYSIS

This research is a quantitative research. This study proposed a method for segmentation of blood vessels in retinal images by combining the image improvement method and the segmentation method. The performance which used to measure the success of the proposed method were accuracy, specificity, and sensitivity.

2.1. Data Collection

The dataset used is derived from STARE data (Structured Analysis of The Retina Dataset) which can be accessed from the following page: https://cecas.clemson.edu/ ahoover/stare/ and DRIVE (Digital Retinal Images for Vessel Extraction) dataset which can be accessed from the following page: https://drive.grand-challenge.org/.

2.2. Method

The steps in the process of image enhancement and segmentation of retinal blood vessels were as follows:

A. Input Image

This process begins by preparing retinal fundus images obtained from the DRIVE and STARE datasets. The input image was an essential step in segmenting blood vessels. Image input can also be referred to as the first step in preparing data to be studied using the proposed method. The DRIVE dataset image had 565 x 584 pixels with 96 dpi, 712 KB in size, and used .tif format. Furthermore, the STARE dataset image had 700 x 605 pixels with 72 dpi, 1.21 MB in size, and used the .ppm format.

B. Image Enhancement

This process was improved retinal image quality due to non-uniform lighting and poor contrast, including unwanted noise. The steps were as follows:

1. Green Channel

   There are three color channels in the original image, namely red, green, and blue. The image obtained from the dataset is an image of type RGB (red, green, blue) which will only take the green channel because the green channel provides maximum contrast between the image and the background. Please note that for information in the image, $C(x, y.1)$ contains information on the red channel matrix components, then $C(x, y.2)$ contains information on the green channel matrix components, and $C(x, y.3)$ contains component information matrix of blue channels [9]. The equations for obtaining a green channel was:

$$G(x, y) = C(x, y.2) \tag{1}$$

   where G is the green channel, C is the retinal image, (x, y) is x represents the rows and y represents columns, and $(x, y.2)$ epresents the rows and columns in the green channel.

2. Contrast Stretching

   Contrast Stretching is one method of improving image quality, which is often done to improve low contrast images that may result from poor lighting quality [3]. For example, s was the gray level value of the image after processing, and r was the gray level value before it was processed. The value points $(r1, s1)$ then $(r2, s2)$ would determine the shape of the transformation and could be set to determine the spread of the gray level of an image. If the curve in the image did not form a straight line, there would be a change in color gradation, in this case, the grayscale. If the point $(r1, s1)$ shifts, there would be a change in the gray color gradient. The Equation obtained from the curve can be seen in Equation (2) [10].

$$s = r\frac{s_1}{r_1}, \text{ jika } 0 \leq r < r_2 \tag{2}$$

$$s = s_1 + \frac{(r - r_1) \times (s_2 - s_1)}{r_2 - r_1}, \text{ jika } r_1 \leq r < r_2 \tag{3}$$

$$s = s_1 + \frac{(r - r_1) \times (255 - s_2)}{255 - r_2}, \text{ jika } r_2 \leq r < 255 \tag{4}$$

   where r is the intensity value of the color to be changed, s is the intensity value that has been changed, (r_1, s_1) is a random intensity value pair with a value range of $0 - 255$, (r_2, s_2) is a random intensity value pair with a value range $0 - 255$, provided that $r_1 < r_2$ and $s_1 < s_2$.

C. Segmentation

One method of segmentation is the Adaptive Thresholding algorithm. The threshold is a simple but effective tool for separating objects from the background [11]. This process was based on the value of the difference gray degrees, where the intensity of the image that is more than or equal to the threshold value would be changed to 1 (white), and values less than the threshold

would be changed to 0 (black). The process taken for the threshold value is using the mean method or known as the adaptive local thresholding mean filter with the following Equation:

$$Z(i,j) = \begin{cases} 1, \text{ if } y(i,j) \geq T \\ 0, \text{ if } y(i,j) < T \end{cases} \tag{5}$$

With the value of T as follows:

$$T = \frac{\Sigma_{(i,j)} \Sigma_{\alpha} f^{(i,j)}}{N_{\alpha}} - C \tag{6}$$

It can be reduced by Equation (7) to become the following Equation:

$$T = \begin{cases} 1, \text{ jika } y(i,j) \geq \dfrac{\Sigma_{(i,j)} \Sigma_{\alpha} f^{(i,j)}}{N_{\alpha}} - C \\ 0, \text{ jika } y(i,j) < \dfrac{\Sigma_{(i,j)} \Sigma_{\alpha} f^{(i,j)}}{N_{\alpha}} - C \end{cases} \tag{7}$$

where T is the thresholding value, Z is the binary value in the image, $y(i,j)$ is the initial value of the image input in the ith row of the jth column, C is a constant value that can be determined freely, α is the total number of pixels that processed, N_{α} is the number of the pixel block α.

D. Post Processing

Furthermore, for the post-processing stage, which helps eliminate noise in the segmentation results, the following steps are carried out:

1 Opening Morphology

Morphology is an image processing technique based on the shape of the image segment, which aims to improve the segmentation results [12]. This operation is handy for representing the shape of the area, such as boundaries, frames, and others. The morphological opening is an erosion process followed by opening dilation, which is usually used to remove small image objects. Erosion operation is a technique to reduce the edge of an object, while dilation is a technique to enlarge an object segment by adding layers around it [13]. Systematically, the Opening morphology equation is as follows:

$$A \circ B = (A \ominus B) \oplus B \tag{8}$$

where A is the original image, B is the element structure, $\circ$ is the Opening morphology operation, $\ominus$ is the erosion operation (the process of removing object points from being part of the background), and $\oplus$ is a dilation operation (the process of merging background points to become part of the object).

2 Median Filter

Median Filter is a filter that looks for the median value by comparing its nearest local area [14]. The general form of the Median Filter is shown in Equation (9) as follows [15].

$$f(x,y) = \text{median}_{(}p,q)(g(p,q)) \tag{9}$$

where $f(x,y)$ is the result of the filter where x and y represent rows and columns, (p,q) denotes the pixel size value, and g is the operator's function.

3 Closing Morphology

Closing morphology is the opposite of the Opening process, namely the dilation process first followed by the erosion

process. The goal is to fill small holes in objects or combine adjacent objects [16]. The Closing morphological equations are as follows:

$$A \bullet B = (A \oplus B) \ominus B \tag{10}$$

where A is the original image, B is the element structure, $\bullet$ is the Closing morphology operation, $\ominus$ is the erosion operation (the process of removing object points from being part of the background), and $\oplus$ is a dilation operation (the process of merging background points to become part of the object).

E. Output Image

The results of image enhancement and segmentation of retinal blood vessels are stored using the ".jpg" format and will be compared with the ground truth of each dataset. The stages of the process of image enhancement and segmentation of retinal blood vessels with an example of the DRIVE dataset with the file name "12_test.tif and STARE with the file name "im0082.ppm" can be seen in Figure 1 below.

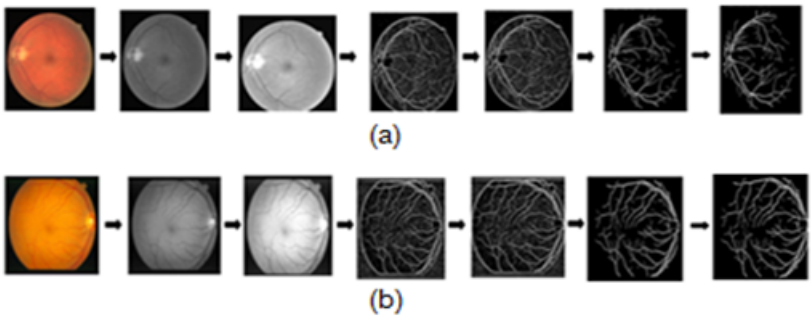

Figure 1. The process of image enhancement and segmentation
(a) DRIVE 12_test.tif (b) STARE im0082.ppm

Based on Figure 1, it can be seen that the image processing process from the initial RGB image is converted into a green channel image. The image enhancement process is carried out using the Contrast Stretching method. Then, the segmentation process is carried out using the Adaptive Thresholding method. Furthermore, the post-processing stage used the Opening morphology, Median Filter, and Closing morphology to eliminate noise. The stages of this retinal blood vessels research were data collection, image enhancement, segmentation, and post preprocessing which can be seen in Figure 2.

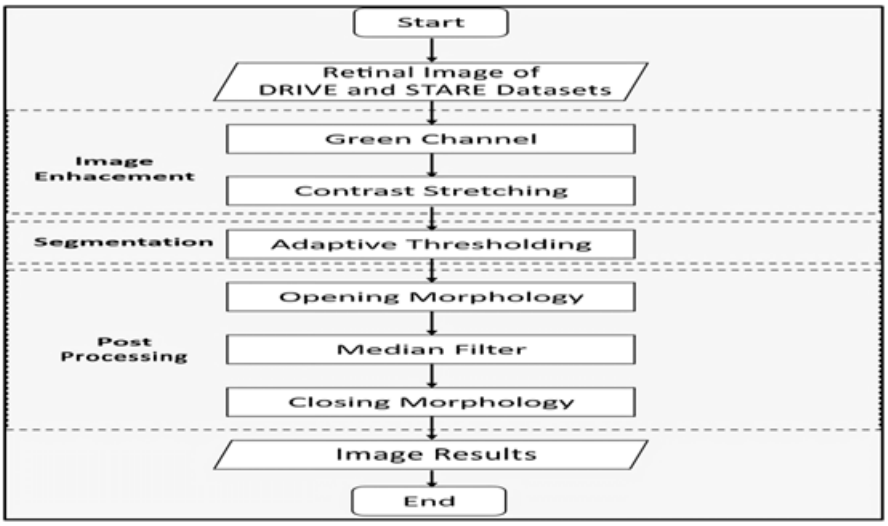

Figure 2. The research flowchart

3. RESULT AND ANALYSIS

3.1. Image Enhancement

An example of image quality enhancement using the Contrast Stretching method can be seen in Figure 3.

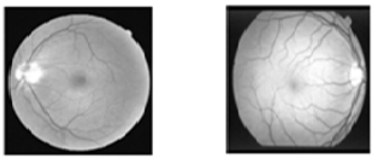

Figure 3. Image quality enhancement results using the Contrast Stretching method
(a) DRIVE 12_test.tif (b) STARE im0082.ppm

The next step was to calculate the PSNR (Peak Signal to Noise Ratio) and MSE (Mean Square Error) values for the evaluation process of improving image quality using the Contrast Stretching method. PSNR is a measure of the level of success in improving image quality. The PSNR value is obtained from the difference between the value of the original image and the resulting image enhancement (improvement of image quality). To find out the PSNR value of an image, what is needed is the MSE value first. The greater the PSNR value, the better the processed image, the image quality resulting from the improvement process is considered high if the PSNR is 40 dB or more [5, 17].

The PSNR and MSE values from the image quality enhancement result from the 20 DRIVE and STARE datasets in Figure 4 and Figure 5.

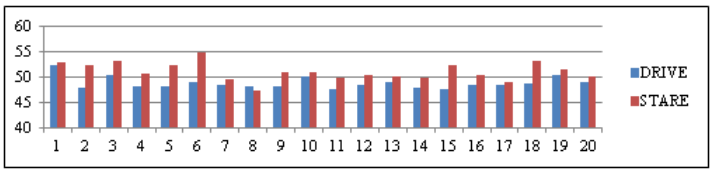

Figure 4. Graph of PSNR values for 20 DRIVE datasets and 20 STARE datasets

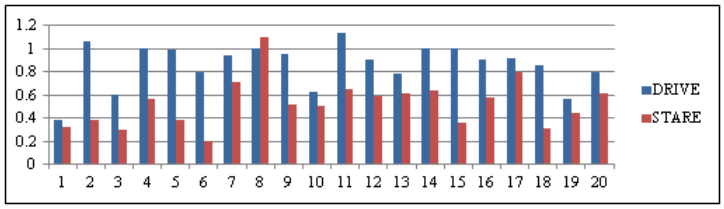

Figure 5. Graph of MSE values for 20 DRIVE datasets and 20 STARE datasets

Based on Figure 4 and Figure 5, the results of image quality enhancement with the DRIVE dataset produced an average MSE value of 0.8720 and a PSNR value of 48.891 dB. Then for the STARE dataset test, the average PSNR value was 48.6716 dB, and the MSE was 0.5360. According to [5], if the PSNR value is $>$ 40 dB from an image, it can be concluded that the image has high quality. This means that the PSNR values obtained from both the DRIVE and STARE datasets have an average of above 40 dB, indicating that the results of the image quality improvement that have been carried out are very good.

From Figures 4 and 5, the image that had the best quality was obtained by the 1st image in the DRIVE dataset with PSNR 52.3476 and MSE 0.3817, while in the STARE dataset, it was received by the 6th image with PSNR 55.0503 and MSE 0.2049. For images that had less good quality than other images obtained by the 11th image in the DRIVE dataset with PSNR 47.5778 and MSE 1.1447, the 8th image received the STARE dataset with PSNR 47.4777 and MSE 1.1714.

3.2. Segmentation

The final result of the segmentation of the proposed method can be seen in Figure 6.

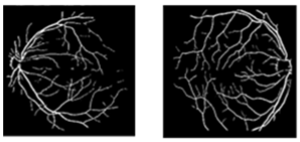

(a) (b)

Figure 6. The final result of segmentation using the Adaptive Thresholding method
(a) DRIVE 12_test.tif (b) STARE im0082.ppm

An example of the results of 10 images of the DRIVE and STARE datasets after the segmentation process stages can be seen in Table 1.

Table 1. Comparison of Ground Truth with Test Results on the DRIVE and STARE datasets

No	File Name	Ground Truth	Hasil	File Name	Ground Truth		Result
					Adam Hoover	Valentina Kouznetsova	
1	01_test.tif	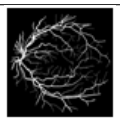		Im0001.ppm	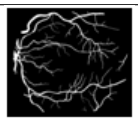	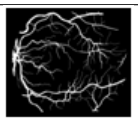	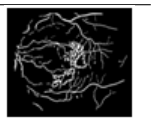
2	02_test.tif			Im0002.ppm		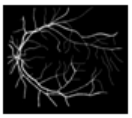	
3	03_test.tif			Im0003.ppm	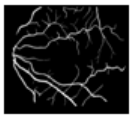	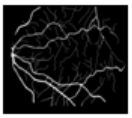	
4	04_test.tif			Im0004.ppm			
5	05_test.tif			Im0005.ppm			
6	06_test.tif			Im0044.ppm			
7	07_test.tif			Im0077.ppm		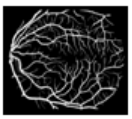	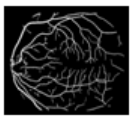
8	08_test.tif			Im0081.ppm		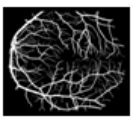	
9	09_test.tif			Im0082.ppm			
10	10_test.tif			Im0139.ppm			

From the final results in Table 1, it can be seen that there were thin blood vessels that were not detected, but all of the thick blood vessels were caught well. The next stage was the evaluation process of the segmentation results. The evaluation results of the proposed method for segmenting blood vessels in retinal images could be calculated using the confusion matrix. The confusion matrix is a tool to measure the suitability of the processed data with the reference data. There were parameters to be calculated in the confusion matrix, namely accuracy, sensitivity, and specificity.

The DRIVE dataset obtained TP=1,125,878, the STARE dataset (Adam Hoover) obtained TP=1,304,286, and the STARE dataset (Valentina Kouznetsova) obtained TP=1,436,190, meaning that the number of blood vessel pixels was correctly predicted in the results segmentation. Furthermore, the values obtained were FP=607,959 in the DRIVE dataset, FP=627,909 in the STARE dataset (Adam Hoover), and FP=1,330,071 in the STARE dataset (Valentina Kouznetsova), meaning the number of pixels of blood vessels that are predicted as non-vessels in the segmentation results. Furthermore, the values obtained are FN=244,563 in the DRIVE dataset, FN=352,080 in the STARE dataset (Adam Hoover), and FN=220,230 in the STARE dataset (Valentina Kouznetsova), meaning the number of non-vessel pixels predicted as blood vessels in the segmentation results. Furthermore, the values obtained are TN=17,819,202 in the DRIVE dataset, TN=23,125,725 in the STARE dataset (Adam Hoover), and TN=22,423,509 in the STARE dataset (Valentina Kouznetsova). The True Negative (TN) value was a number of negative data (as background pixel) that was detected correctly, while False Positive (FP) was a number of negative data (as background pixel) but detected as positive data (as retinal blood vessel). Meanwhile, True Positive (TP) was positive data (as retinal blood vessel pixela) that was detected correctly. False Negative (FN) was the opposite of True Positive (TP). The results had meaning that the number of background pixels was predicted correctly. The performance evaluation results of the proposed method for segmentation of blood vessels, including the values of accuracy, sensitivity, and specificity for each image, can be seen in Figure 7, Figure 8, and Figure 9.

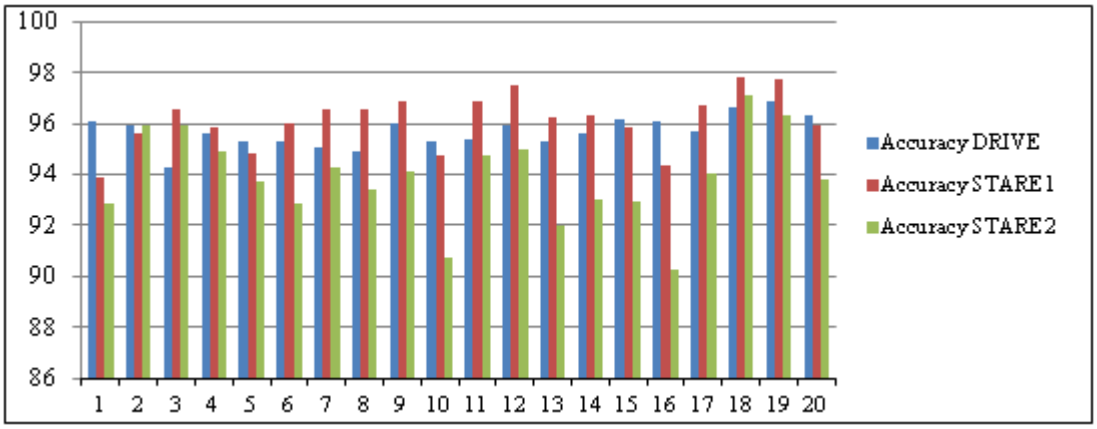

Figure 7. Graph of accuracy values for 20 DRIVE datasets and 20 STARE datasets

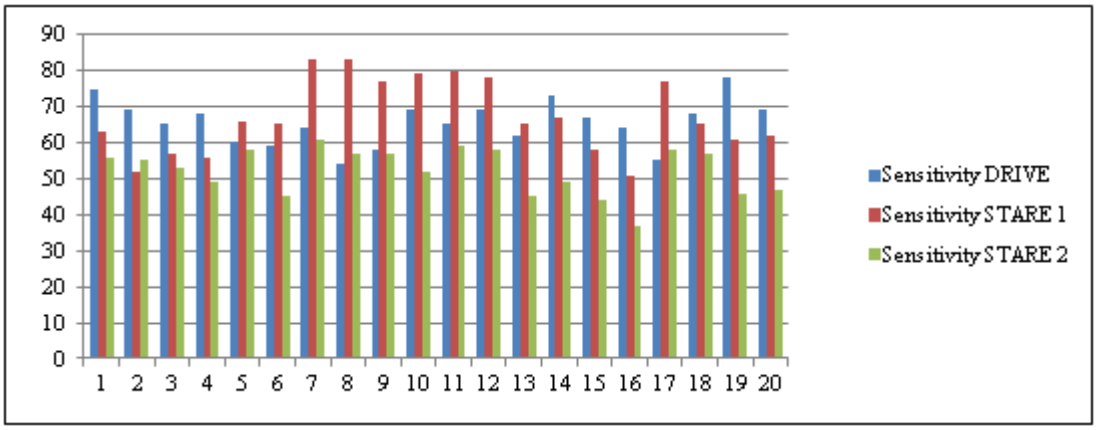

Figure 8. Graph of sensitivity values for 20 DRIVE datasets and 20 STARE datasets

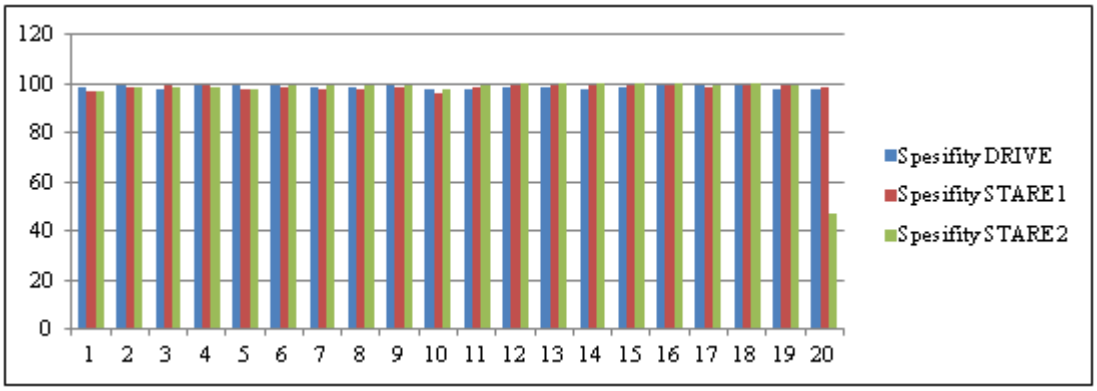

Figure 9. Graph of specificity values for 20 DRIVE datasets and 20 STARE datasets

Figure 7, Figure 8, and Figure 9 are the results of comparing the segmentation results with the ground truth of the DRIVE and STARE datasets. In the DRIVE dataset, the average accuracy was 95.68%, the sensitivity was 65.05%, and the specificity was 98.56%. The STARE dataset with Adam Hoover's ground truth resulted in an average accuracy of 96.13%, sensitivity of 65.90%, and specificity of 98.48%. The ground truth comparison of Valentina Kouznetsova yielded an average value of 93.89% accuracy, 52.15% sensitivity, and 99.02% specificity.

Based on Figure 7, it can be seen that the highest accuracy value was obtained by the 19th image of 96.9% in the DRIVE dataset. In comparison, in the STARE dataset with the ground truth of Adam Hoover and Valentina Kouznetsova, it was obtained by the 18th image of 97.81% and 97.12%, respectively. This shows that the segmentation prediction results on the image almost resemble the ground truth. The lowest accuracy value was achieved by the 3rd image of 94.30% on the DRIVE dataset, in the STARE dataset with Adam Hoover's ground truth obtained by the 1st image of 93.89%. In contrast, the STARE dataset with Valentina Kouznetsova's ground truth was received by the 16th image by 90.25%.

In Figure 8, the highest sensitivity value obtained by the 19th image was 78% in the DRIVE dataset, while in the STARE dataset using the ground truth of Adam Hoover and Valentina Kouznetsova, it was obtained by the 7th image of 83% and 61%, respectively. This indicates that thin blood vessels can be detected well. The lowest sensitivity value was achieved by the 3rd image of 94.30% in the DRIVE dataset. In contrast, the STARE dataset with ground truth Adam Hoover and Valentina Kouznetsova obtained it by the 16th image of 51% and 37%, respectively.

Based on Figure 9, the highest specificity value was obtained by the 4th image of 99.47% in the DRIVE dataset, in the STARE dataset with Adam Hoover's ground truth obtained by the 18th at 99.54%, while in STARE with Valentina Kouznetsova's ground truth obtained by the 12th image at 99.88%. This shows that the segmented image did not have a lot of noise. For the lowest specificity value achieved by the 3rd image of 97.56% in the DRIVE dataset, in the STARE dataset with Adam Hoovers ground truth obtained by the 19th at 96.13%, while in STARE with Valentina Kouznetsovas ground truth obtained by the 1st image at 96.61%.

3.3. Result Comparison

The comparison of processing results with other studies can be seen in Table 2.

Table 2. Comparison of processing results with other research

Method	Accuracy (%)	Sensitivity (%)	Spesifisity (%)
DRIVE Dataset			
Frangi Filter + Otsu thresholding [7]	**96,58**	46,55	97,03
CLAHE dan Adaptive Filter + Otsu thresholding [10]	93,68	61,60	96,77
CLAHE dengan Average dan Gaussian Filters + ISODATA [10]	95,10	60,27	98,46
Hessian Matrix + Random walks [8]	93,76	63,33	98,24
Morphological hit-or-miss transform [18]	94,31	61,29	97,44
Proposed Method DRIVE	95,68	**65,05**	**98,56**
STARE Dataset			
Frangi Filter + Otsu thresholding [7]	93,76	49,7	94,08
CLAHE dan *Adaptive Filter + Otsu thresholding* [10]	94,56	61,35	97,22
CLAHE dengan *Average* dan *Gaussian Filters* + ISODATA [10]	94,71	61,27	97,40
2D-Gabor Filter + Adaptive Thresholding [9]	91,00	36,00	97,00
Proposed Method 1 STARE	**96,13**	**65,90**	98,48
Proposed Method 2 STARE	93,89	52,15	**99,02**

Table 2 shows a comparison of the results of accuracy, sensitivity, and specificity obtained from the proposed method with other studies in the DRIVE and STARE datasets. In contrast, using the DRIVE dataset, the highest accuracy value was achieved by [7] research which applied Otsu Thresholding with image improvement using the Frangi filter. Still, the sensitivity value was lower than other methods using the DRIVE dataset. The highest sensitivity and specificity values were obtained by the proposed method. The proposed method received the highest accuracy and sensitivity values in the STARE dataset using Adam Hoover's ground truth.

In contrast, the proposed method used Valentina Kouznetsova's ground truth to achieve the highest specificity value. Based on the results of the performance evaluation of the proposed method, it can be concluded that the accuracy of the proposed method in segmenting blood vessels is outstanding, indicated by an accuracy value of 95.68% in the DRIVE dataset and the STARE dataset of 96.13% and 93.89%, respectively. In addition, the proposed method's ability to correctly predict blood vessel pixels is quite good, as indicated by the sensitivity values of 65.05% in the DRIVE dataset and 65.90% and 52.15% in the STARE dataset, respectively. Furthermore, the ability of the proposed method to correctly predict non-vessel pixels is outstanding, indicated by the specificity values of 98.56% in the DRIVE dataset and the STARE dataset of 98.48% and 99.02%, respectively.

4. CONCLUSION

The results of image quality enhancement that have been carried out are outstanding because they can produce high image quality with values above 40 dB. The segmentation results on the DRIVE and STARE datasets yielded a high average accuracy value, a reasonably good sensitivity value, and a high specificity. The proposed method's ability to predict thick blood vessels is outstanding. However, some have still not been detected for thin blood vessels, and the ability to predict a black background with white sample classification is exceptional. This study enhances image quality and segmentation of retinal blood vessels using Contrast Stretching and Adaptive Thresholding methods. However, the sensitivity results are still low. So it is hoped that further research can increase the sensitivity value and predicts fine blood vessels. This study provided an alternative method that was valid and accurate enough to be used in improving blood vessel segmentation images at once. if the image segmentation resulted have good quality then the image could be used in the cla ssification of retinal disorders.

5. ACKNOWLEDGEMENTS

The Acknowledgments section is optional. Research sources can be included in this section.

6. DECLARATIONS

AUTHOR CONTIBUTION

FUNDING STATEMENT

COMPETING INTEREST

REFERENCES

[1] S. Qummar, F. G. Khan, S. Shah, A. Khan, S. Shamshirband, Z. U. Rehman, I. A. Khan, and W. Jadoon, "A Deep Learning Ensemble Approach for Diabetic Retinopathy Detection," *IEEE Access*, vol. 7, pp. 150 530–150 539, 2019.

[2] K. Naveed, F. Abdullah, H. A. Madni, M. A. Khan, T. M. Khan, and S. S. Naqvi, "Towards Automated Eye Diagnosis: An Improved Retinal Vessel Segmentation Framework Using Ensemble Block Matching 3d Filter," *Diagnostics*, vol. 11, no. 1, pp. 1–27, 2021.

[3] Murinto, S. Winiarti, D. P. Ismi, and A. Prahara, "Image enhancement using piecewise linear contrast stretch methods based on unsharp masking algorithms for leather image processing," *Proceeding - 2017 3rd International Conference on Science in Information Technology: Theory and Application of IT for Education, Industry and Society in Big Data Era, ICSITech 2017*, vol. 2018-Janua, pp. 669–673, 2017.

[4] E. Erwin and D. R. Ningsih, "Improving Retinal Image Quality Using The Contrast Stretching, Histogram Equalization, and CLAHE Methods with Median Filters," *International Journal of Image, Graphics and Signal Processing*, vol. 12, no. 2, pp. 30–41, 2020.

[5] N. Chervyakov, P. Lyakhov, D. Kaplun, D. Butusov, and N. Nagornov, "Analysis of The Quantization Noise in Discrete Wavelet Transform Filters for Image Processing," *Electronics (Switzerland)*, vol. 7, no. 8, 2018.

[6] H. Michalak and K. Okarma, "Region based adaptive binarization for optical character recognition purposes," *2018 International Interdisciplinary PhD Workshop, IIPhDW 2018*, pp. 361–366, 2018.

[7] O. Ali and N. Muhammad, "A comparative study of automatic vessel segmentation algorithms," in *3rd International Conference on Computing, Mathematics and Engineering Technologies (iCoMET)*, 2020, pp. 1–6.

[8] T. Mapayi, S. Viriri, and J.-r. Tapamo, "Comparative Study of Retinal Vessel Segmentation Based on Global Thresholding Techniques," *Computational and Mathematical Methods in Medicine*, vol. 2015, pp. 1–15, 2015.

[9] Y. Li, H. Gong, W. Wu, G. Liu, and G. Chen, "An Automated Method Using Messian Matrix and Random Walks for Retinal Blood Vessel Segmentation," *Proceedings - 2015 8th International Congress on Image and Signal Processing, CISP 2015*, vol. 1, no. Cisp, pp. 423–427, 2016.

[10] A. Desiani, D. A. Zayanti, R. Primartha, F. Efriliyanti, and N. A. C. Andriani, "Variasi Thresholding untuk Segmentasi Pembuluh Darah Citra Retina," *Jurnal Edukasi dan Penelitian Informatika JEPIN*, vol. 7, no. 2, pp. 255–262, 2021.

[11] A. Akagic, E. Buza, and S. Omanovic, "Pothole Detection: An Efficient Vision Based Method Using RGB Color Space Image Segmentation," *2017 40th International Convention on Information and Communication Technology, Electronics and Microelectronics, MIPRO 2017 - Proceedings*, pp. 1104–1109, 2017.

[12] Vargaz vazques D, R. r. J, and J. A. R. Shancez, "Face segmentation using mathematical morphology on single faces," *IEEE*, pp. 3–6, 2016.

[13] Nurliadi, P. Sihombing, and M. Ramli, "Analisis Contrast Stretching Menggunakan Algoritma Euclidean Untuk Meningkatkan Kontras Pada Citra Berwarna," vol. 03, no. 2013, pp. 26–38, 2016.

[14] U. Erkan, L. Gökrem, and S. Enginolu, "Different applied median filter in salt and pepper noise," *Computers and Electrical Engineering*, vol. 70, pp. 789–798, 2018.

[15] M. A. Díaz-Cortés, N. Ortega-Sánchez, S. Hinojosa, D. Oliva, E. Cuevas, R. Rojas, and A. Demin, "A multi-level thresholding method for breast thermograms analysis using Dragonfly algorithm," *Infrared Physics and Technology*, vol. 93, no. August, pp. 346–361, 2018.

[16] X. Yan, M. Jia, W. Zhang, and L. Zhu, "Fault Diagnosis of Rolling Element Bearing Using A New Optimal Scale Morphology Analysis Method," *ISA Transactions*, vol. 73, pp. 165–180, 2018.

[17] W. Lilik, R. Imam, and P. Yudi, "Comparative Analysis of Image Steganography using SLT,DCT and SLT-DCT Algorithm," *Matrik : Jurnal Manajemen, Teknik Informatika dan Rekayasa Komputer*, vol. 20, no. 1, pp. 169–182, 2020.

[18] S. Pal, S. Chatterjee, D. Dey, and S. Munshi, "Morphological operations with iterative rotation of structuring elements for segmentation of retinal vessel structures," *Multidimensional Systems and Signal Processing*, vol. 30, no. 1, pp. 373–389, 2019.